Journal of Catalysis **183,** 6–13 (1999)
Article ID jcat.1998.2375, available online at http://www.idealibrary.com on IDEAL®

Pt–TiO_2–γ Al_2O_3 Catalyst

I. Dispersion of Platinum on Alumina-Grafted Titanium Oxide

Neuman Solange de Resende,*[,1] Jean-Guillaume Eon,† and Martin Schmal*[,‡]

*NUCAT/PEQ/COPPE, Federal University of Rio de Janeiro, Rio de Janeiro, Brazil; †Instituto de Química, Federal University of Rio de Janeiro, Rio de Janeiro, Brazil; and ‡Escola de Química, Federal University of Rio de Janeiro, Rio de Janeiro, Brazil

Received January 29, 1997; revised November 25, 1998; accepted December 1, 1998

Polymeric titanium oxides grafted on γ-Al_2O_3 were used as supports for platinum catalysts containing 1 wt.% Pt. The supports were prepared from an interaction of alumina with titanium isopropoxide, impregnated with hexachloroplatinum acid (H_2PtCl_6) and calcined at 773 K. Pure alumina and titania were used for comparison. The solids were characterized by XRD, TPR, DRS-UV-vis, and TEM. Frontal hydrogen chemisorption was measured after TPR. CO adsorption isotherms were recorded after reduction at low (573 K) and high (773 K) temperature. The results indicate that the polymeric titanium oxide layer in the catalyst, although reducible under hydrogen at high temperature, does not promote a strong metal–support interaction effect. Platinum dispersions in the titania-modified catalysts are higher than in alumina catalysts.

INTRODUCTION

Noble metals are currently combined in exhaust catalysts in order to reduce carbon monoxide and nitrogen oxide levels. However, recent attempts have shown that it is possible to substitute costly metals such as rhodium by promoters in the oxide form. Similar performances to that of a Rh catalyst, for example, have been obtained with nonconventional additives such as MoO_3 (1, 2). It is known that transition metal oxides are easily reducible and strongly interact with metals of group VIII. Strong metal–support interaction (SMSI) in Pt–TiO_2 catalysts was extensively studied (3–7). The effect has been observed for titania-supported platinum catalysts as well as for platinum supported on titanium oxide dispersed over an alumina support and is known to affect catalytic properties by decreasing the adsorption capacity of the metal. It has been demonstrated that the main effect is a geometric one; blockage of superficial metal atoms occurs due to migration of the metal oxide at high temperature reduction (7).

Other milder metal–support interactions have been postulated to interpret the promoter effect of titania in some conditions where SMSI is not present. Enhancement of catalytic properties could occur at the interface between the metal particle and the transition metal oxide (7). There is, however, some confusion in the literature regarding a close distinction of the various effects and more work is needed to achieve full understanding.

Titanium dioxide is a nonstoichiometric phase (8) which could be used for oxygen storage in exhaust catalysts. We have shown in a previous work (9) that grafting methods lead to the formation of thermally stable, bidimensional titanium oxide layers over γ-alumina supports. We show here that these materials can be used as new supports on which to disperse platinum. It is shown that the catalyst is highly stabilized against SMSI effects and moreover that high platinum dispersions are attained.

METHODS

A. *Preparation of the Catalysts*

Three different supports were chosen for comparison: γ-alumina (Harshaw, Al 3996) was used in powder form after calcination under air flow (4 h, 5 K/min) at 1073 (A1) and 873 K (A2). Titanium dioxide (anatase) was obtained from hydrolysis of titanium isopropoxide (Aldrich, 97%) and calcined at 803 K. The surface areas of these materials were 157, 188, and 88 m^2/g, respectively. Titanium-modified aluminas, TiO_x–γ-Al_2O_3, were prepared following two different methods, as previously reported (9–11). The grafting method was applied in order to achieve titanium oxide monolayers over γ-Al_2O_3: two solids were prepared with different titanium nominal loadings: 5 wt.% equivalent TiO_2 over A1 (TA5) and 10 wt.% equivalent TiO_2 over A2 (TA10). Therefore, a nonaqueous solution of titanium isopropoxide in tetrahydrofuran (THF) was added to dry alumina and kept under argon atmosphere for 24 h. The solids were washed with THF before drying. To get a higher loading of titanium oxide (18 wt.% equivalent TiO_2), the dry impregnation method was used with the same solution and support A1. These three supports (TAx, $x = 5$, 10, 18)

[1] To whom correspondence should be addressed.

0021-9517/99 $30.00

were dried at 393 K and calcined under air flow at 773 K for 4 h.

Platinum was impregnated on bulk titania (PT), alumina A1 (PA), and titanium-modified aluminas (PTAx, $x = 5, 10, 18$) by using hexachloroplatinum acid solution. The nominal concentration of platinum was 1 wt.% in the five catalysts. These were dried at 393 K and calcined under air flow at 773 K for 4 h. For the sake of clarity, we reserve the term titania to describe bulk titanium dioxide in the PT catalyst whereas polymeric titanium oxide layers stands for alumina-grafted titanium oxides in PTAx catalysts ($x = 5, 10$).

B. Sample Characterizations

Chemical analysis was performed with a Perkin–Elmer 1200B atomic absorption apparatus, while surface area and pore volumes were measured with an ASAP 2000 Micromeritics apparatus.

Temperature programmed reduction (TPR) and hydrogen chemisorption were performed in a dynamic apparatus described elsewhere (11). The reducing mixture was 1.7% H_2–Ar, flowing at 30 ml/min over 1 g of catalyst. The sample was dried previously by flowing Ar at 423 K for 30 min. For TPR, the temperature was then raised at a heating rate of 10 K/min from 298 K up to 803 K. The final temperature of reduction was held constant for 1 h. Then, the sample was cooled to RT under Ar flow for 30 min and the valve switched to H_2–Ar mixture to proceed to the frontal chemisorption (total and reversible).

The volumetric chemisorption of CO by static method was performed in an ASAP 2000 "Chemi System" Micromeritics. The sample (0.5 g) was dried at 393 K for 30 min and then reduced with a flowing mixture of 2% H_2–Ar at 573 K for 1 h. After evacuation and cooling at 303 K, CO uptakes were measured varying the pressure in the range between 50 to 320 mm Hg. Total and reversible adsorption isotherms were recorded. The same procedure was used after reduction at 773 K. Blank adsorption experiments for the support material were also performed. The dispersions were calculated assuming linear CO bonding and unit cells corresponding to 1.25×10^{19} Pt atoms/m^2.

TEM measurements were performed in a JEOL JEM-2000FX apparatus. EDS analysis was obtained by using a spectroscopic Tracor Northern 2000 system. The samples, previously reduced at 773 K, were passivated under 2% O_2–He flow at 78 K for 30 min and, raising the temperature to 298 K, for an additional 15 min. Particle diameters were measured using the dark field enlargements micrographs and counting over 200 particles.

UV-visible diffuse reflectance spectra (DRS) were obtained by using a double Varian CARY-5 apparatus for oxide and passivated samples (after reduction). The spectra were obtained at RT in the range of 200–800 nm, using Herrick diffuse reflectance accessory with Praying Mantis geometry and using the support as a reference. The reflectance spectrum is presented according to the Schulz–Munk–Kubelka equation.

X-ray diffraction was performed at RT with a Freiberger–Präzisionsmechanik diffractometer using graphite-monochromated Cu $K\alpha$ radiation. The samples were analyzed in the oxide form.

RESULTS

Table 1 presents the surface areas and pore volumes of the different catalysts together with the corresponding titanium and platinum concentrations measured by chemical analysis. As shown, the surface area and pore volume slightly decrease with increasing the titanium loading. The alumina support (A2) used for the preparation of the PTA10 sample was calcined at 873 K in order to keep a higher density of hydroxyls at the surface, which explains the higher surface area measured for this catalyst.

X-Ray Diffraction

Figure 1 displays the XRD patterns of the Pt catalysts supported on γ-Al_2O_3 (PA), TiO_2 (PT), and titania-modified aluminas (PTAx, $x = 5, 10, 18$). The XRD pattern of the PT catalyst shows well-defined peaks corresponding to the anatase structure and, in particular, the characteristic (101) plane at $2\theta = 25^\circ$. The pattern of the impregnated catalyst (PTA18) shows only a discrete peak at this position.

TABLE 1

Textural Properties of the Platinum Catalysts

Catalysts	Samples	% TiO_2 on support (% wt)[a]	Preparation method of TiO_2–Al_2O_3	BET (m^2/g)	Vp (cm^3/g)	dp (Å)
Pt–Al_2O_3	PA	—		161.4	0.60	147
Pt–5%TiO_2–Al_2O_3	PTA5	4.1	grafted	152.4	0.50	131
Pt–10%TiO_2–Al_2O_3	PTA10	9.7	grafted	176.5	0.53	120
Pt–18%TiO_2–Al_2O_3	PTA18	18.9	impregnated	147.0	0.41	112
Pt–TiO_2	PT	100.0		75.7	0.20	105

[a] Atomic absorption data.

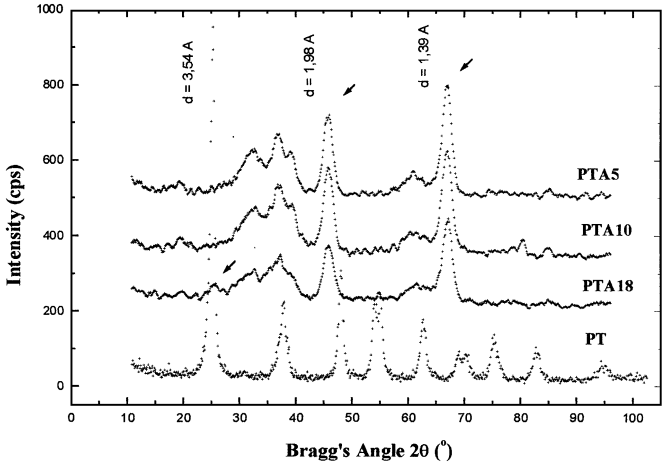

FIG. 1. XRD patterns for 1% platinum catalysts.

However, the patterns of the grafted catalysts only display wide peaks corresponding to the (400) and (440) planes of the support γ-Al_2O_3 ($2\theta = 46^\circ$ and 67°, respectively), which then decrease as the titanium content increases. These results confirm that the catalysts with lower titanium contents (up to 10%) did not exhibit TiO_2 crystallites. The sensibility was low for detecting platinum crystallites at lower contents. However, in this case it seems that particle sizes are less than 5 nm on both oxide and passivated form. This value is the lower detection limit in XRD and is compatible with the results reported below.

UV–Diffuse Reflectance Spectroscopy (UV-DRS)

The DRS spectra of calcined and passivated catalysts are presented in Figs. 2 and 3, respectively. Due to the low platinum content of the samples, the spectra show bands of weak intensity. Arbitrary units were used and no quantitative analysis was attempted. Detailed assignments of the uv-vis spectra of octahedral platinum (IV) complexes in nonaqueous solutions were made by Swihart *et al.* (12). The spectra of superficial complexes formed during calcination under oxygen of $[PtCl_6]^{2-}$ adsorbed on alumina were interpreted later by Liestz *et al.* and Lieske *et al.* (13, 14). In agreement with their results, the spectrum corresponding to the PA sample in Fig. 2 presents an intense absorption at high energy with a shoulder at about 250 nm, which was assigned to charge transfer from chloride ligands to platinum (LMCT) in oxychloride surface complexes $[PtO_xCl_y]$s; we notice for comparison that the corresponding band appears at 262 nm in $[PtCl_6]^{2-}$ complexes (15). This shoulder is observed again in the PTA5 catalyst but not for higher titanium loading, indicating substitution of chloride by oxygen ligands in the platinum coordination sphere. The bands observed at 325, 340, 387, and 412 nm in the spectrum of calcined samples were attributed to *d–d* transitions (13). Bands in the range between 325 and 350 nm are displayed by a great number of superficial platinum (IV) complexes and are thus difficult to attribute (13, 15). However, it is known that the bulk compound $PtO_2 \cdot H_2O$ is characterized by a *d–d* transition band at 425 nm (13). Moreover, this compound is easily reducible. Anticipating the TPR results that showed reduction of the PT catalyst at RT, the band at 412 nm observed for this sample was attributed to this bulk platinum (IV) oxide. In order to account for TPR results, the band at 387 nm in PTA18 catalysts was tentatively attributed to a similar, easily reducible bulk oxide compound.

DRS profiles of the passivated PTA5 and PT catalysts are displayed in Fig. 3. The tail that appears is probably due to the presence of metallic platinum which is not observed on the calcined catalyst. The PT catalyst was not modified after passivation and also contained metallic platinum.

Temperature Programmed Reduction

The TPR profiles of the catalysts are displayed in Fig. 4. The hydrogen consumption is indicated in Table 2 and corresponds to the reduction from Pt^{4+} to Pt^0. The PA

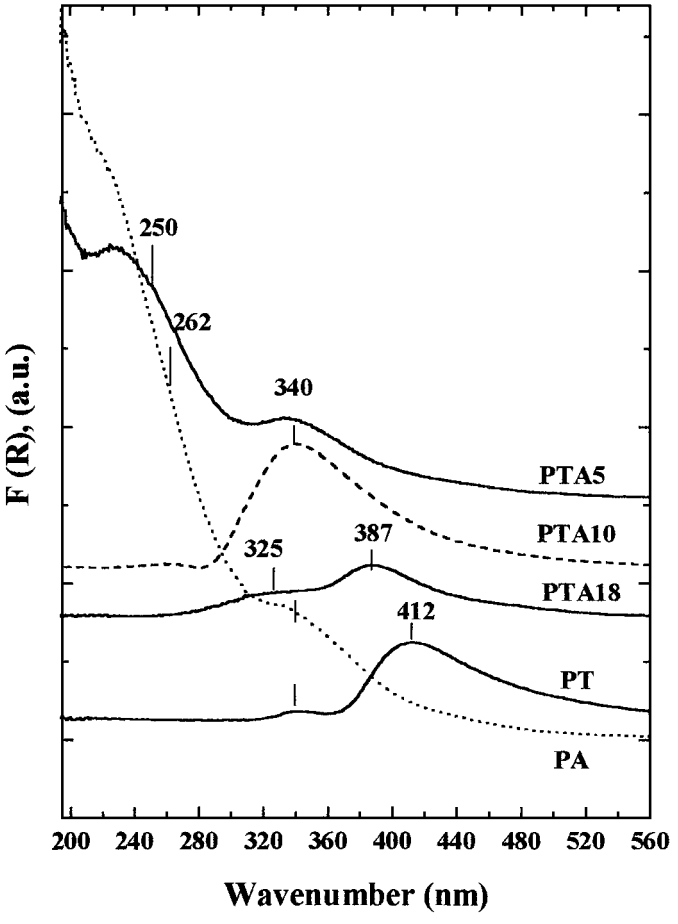

FIG. 2. DRS-UV_{vis} spectra of 1% Pt catalysts, calcined at 823 K, supported on Al_2O_3 (PA), TiO_2 (PT), and 5, 10, and 18% TiO_2–Al_2O_3 (PTA5, PTA10, PTA18).

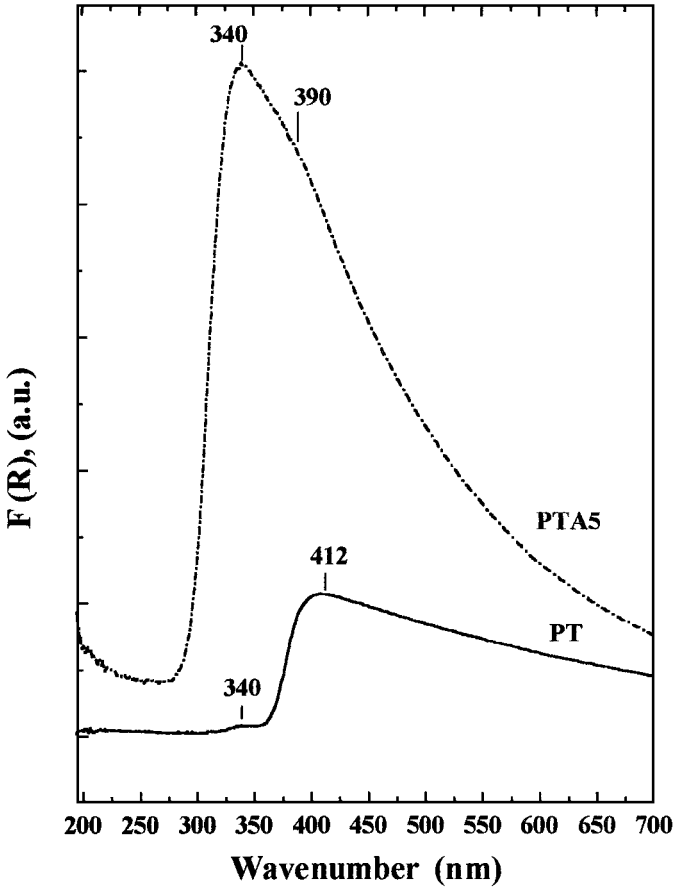

FIG. 3. DRS-UV_{vis} spectra of 1% platinum catalysts supported on TiO_2 (PT) and 5% TiO_2–Al_2O_3 (PTA5), after reduction (803 K) and passivation.

catalyst, used as a reference, shows one well-defined peak at 520 K with a shoulder at 640 K, in good agreement with the literature (4, 14, 16). The hydrogen consumption was slightly lower (82%) than expected for this sample because of partial reduction of platinum already after calcination. On the other hand, the PT catalyst shows four reduction peaks at RT, 385 and 645 K, and above 773 K, where the main peak is shifted toward lower temperature in comparison with the PA sample. It is well known that TiO_2 is partially reduced to TiO_{2-x} under hydrogen at high temperatures (above 773 K); according to the literature (3–7), this reduction is at the origin of the SMSI effect. In agreement with these observations, the high hydrogen consumption seen in Table 2 suggests partial reduction of the titania support during TPR.

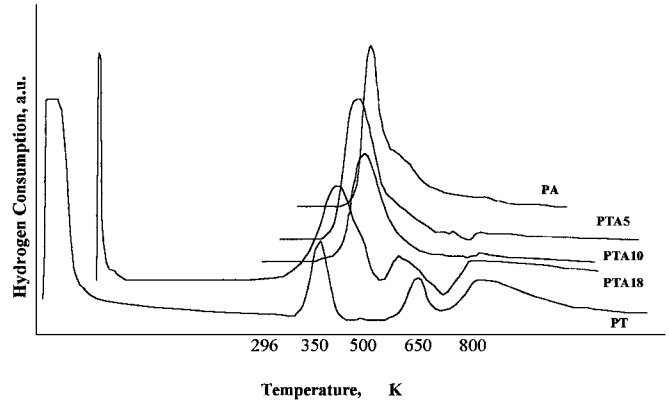

FIG. 4. TPR profiles of catalysts with 1% of platinum supported on Al_2O_3 (PA), TiO_2 (PT), and 5, 10, and 18% TiO_2–Al_2O_3 (PTA5, PTA10, PTA18).

TABLE 2

H_2 Consumption by TPR and by Frontal Chemisorption

Samples	% Pt[a] (wt)	TPR μmol-H_2/gcat	H_2 chemisorption[b] μmol-H_2/gcat	H/M
PA	1.01	84.7[c]	13.9	0.54
PTA5	1.05	158.8	22.0	0.82
PTA10	0.91	129.5	23.4	1.00
PTA18	1.02	151.0	12.0	0.46
PT	1.03	182.9	4.4	0.17

[a] Atomic absorption data.
[b] At 300 K.
[c] Considering 82% of reduction.

The TPR profiles of platinum over titanium oxide sublayers, PTA5 and PTA10, are very similar to the previous one. However they do not display any reduction at RT and the main peak is shifted from 520 to 500 K. The hydrogen consumption indicates that the coated titanium oxide over alumina has also been reduced. Finally, the impregnated catalyst (PTA18) seems to follow more closely the PT catalyst, with the main peak slightly shifted to higher temperature, a small reduction at RT, and a pronounced reduction above 773 K.

The hydrogen uptakes and dispersions measured by frontal chemisorption are also shown in Table 2. It can be seen that platinum is highly dispersed in samples PTA5 and PTA10, even after reduction at high temperature (803 K) during TPR. The high H/M ratios after reduction indicate that SMSI effects were absent in these catalysts. These results are discussed more thoroughly after the exposition of CO chemisorption data.

CO Chemisorption

Results of irreversible CO uptakes are listed in Table 3. Figures 5 and 6 display the total and reversible CO adsorption isotherms of the PTA10 and PTA18 catalysts, respectively. Blank experiments confirmed that CO is not adsorbed on pure titania and polymeric titanium oxide layers supported over alumina after reduction at 573 K. The CO uptake of the 573 K reduced PTAx ($x = 5$, 10, 18) samples increases by a factor of two when compared with the

TABLE 3

Irreversible CO Uptake at 303 K (Static Method)

	Volume of CO adsorbed (μmoles/g)		CO/M	
	Temperature of reduction (K)			
Samples	573	773	573	773
TA10	0.61	—	—	—
TiO_2	0.43	—	—	—
PA	19.11	16.73	0.38	0.33
PTA5	35.61	28.90	0.66	0.54
PTA10	40.71	32.75	0.87	0.70
PTA18	34.33	24.91	0.66	0.48
PT	42.08	13.05	0.80	0.25

PA catalyst. The dispersions of the PT and PTA x ($x = 5$, 10, 18) catalysts are thus about twice that of the PA catalyst.

After reduction at 773 K, the CO uptake of the PT sample strongly decreases indicating the SMSI effect, in agreement with the literature. Although a small decrease is observed for PA and PTA x ($x = 5, 10$) samples, it cannot be attributed to the SMSI effect. The small variation rather suggests that morphology changes of the platinum crystallites could occur at high temperature on these supports. Thus, alumina-grafted titanium oxides provide a stable support for platinum catalysts.

The CO/M ratios after reduction at 773 K may now be compared with the H/M ratios given by frontal hydrogen chemisorption after TPR. Although the values are not in very good agreement, the same trends can be noted. More particularly, the PTA18 catalyst gave H/M and CO/M ratios intermediate between the values observed for PTA5 and PT. This might be attributed to the occurrence of some partial SMSI effect in this catalyst, due to the presence of bulk titania in the support, as was noted earlier from XRD patterns.

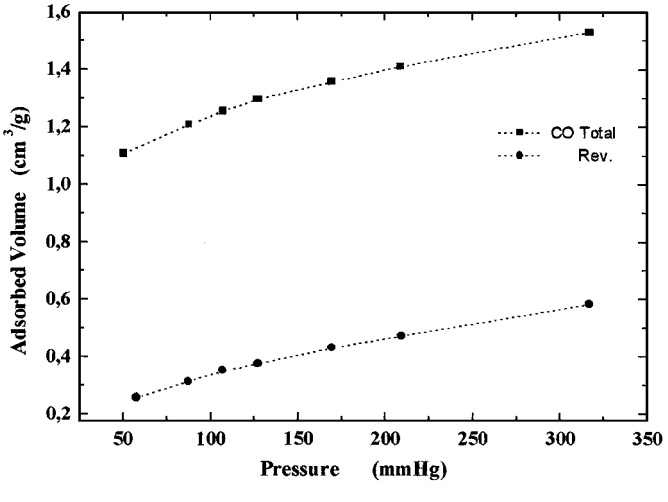

FIG. 5. Adsorption isotherms of CO on 1% Pt–10% TiO_2–Al_2O_3 at 303 K, after reduction at 573 K.

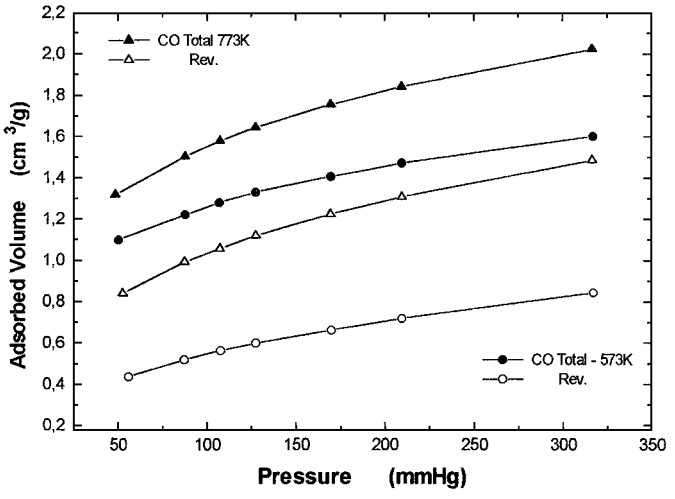

FIG. 6. Adsorption isotherms of CO on 1% Pt–18% TiO_2–Al_2O_3 at 303 K, after reduction at 573 K and 773 K.

Transmission Electron Microscopy

The TEM results were obtained after reduction at 773 K and passivation of the samples. Figure 7 displays the micrographs corresponding to the PTA10 catalyst. The technique of dark and light fields was used allowing identification of metal particles (light points). Figure 8a shows a typical electron diffraction pattern, where all diffraction rings were assigned to the alumina crystallographic planes. The results show that the titanium oxide sublayer is amorphous and well dispersed on alumina. Similar observations were obtained for the PTA5 catalyst. It was already confirmed by EDS (17) that the titanium oxide layer is homogeneously dispersed for titanium loading up to 10 wt.%. On the other hand, the electron diffraction pattern of the PTA18 sample, shown in Fig. 8b, displays an extra diffraction ring which is assigned to the anatase (101) plane. Figure 9 shows a TEM micrograph of this sample which exhibits big platinum particles (5 nm).

Table 4 presents the mean particle sizes calculated from CO chemisorption and TEM results. Almost all values are less than 5 nm, justifying the absence of XRD peaks corresponding to the platinum phase. With the exception of the PT and PTA18 samples, the values are in good agreement. This suggests that the size increase noted earlier, from low to high reduction temperature and occurring for alumina and alumina-grafted titanium oxides, should be real.

The micrographs and EDS results of the elemental analysis for PT and PA catalysts are in good agreement with the literature (18). The PT catalyst exhibits very small particles. EDS result indicates one small platinum peak. The electron diffraction pattern of the PA catalyst displays well-defined rings which are assigned to the (hkl) planes of γ-Al_2O_3 (19).

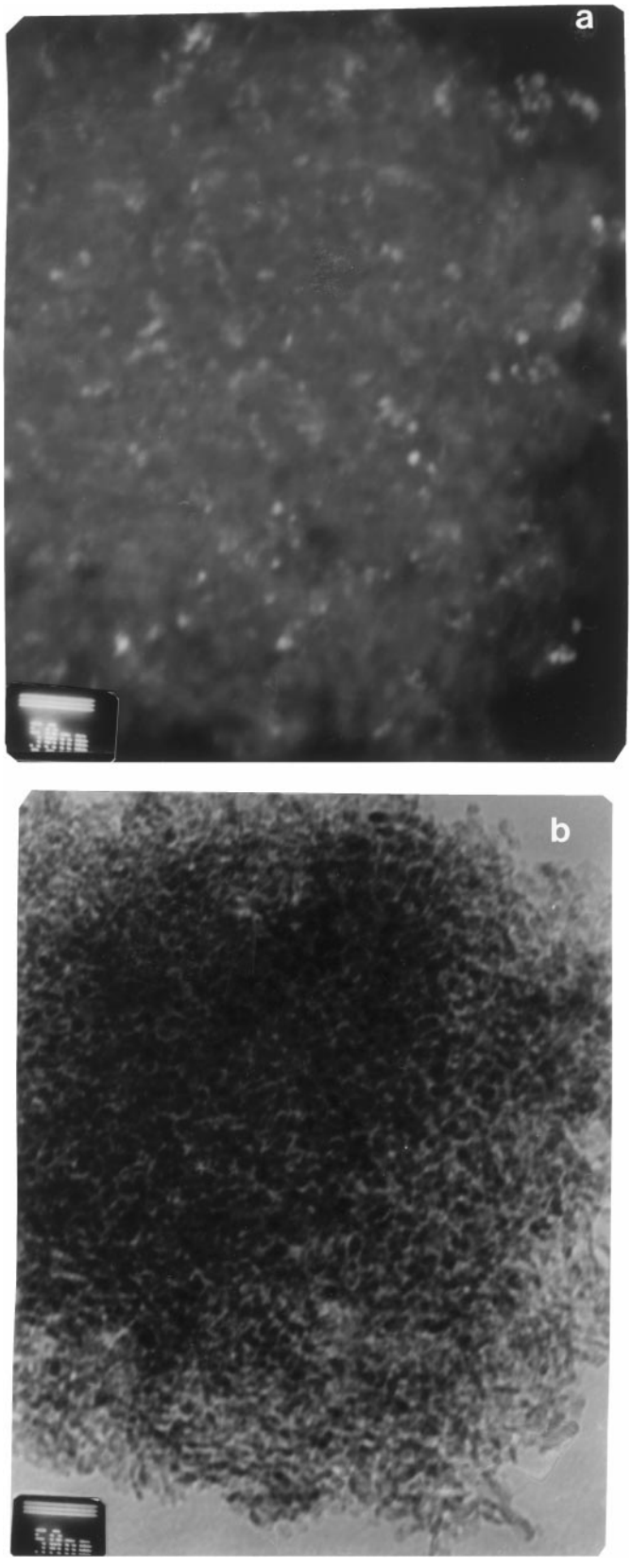

FIG. 7. The transmission micrographs of the 1% Pt–10% TiO_2–Al_2O_3 catalyst. Technique of (a) dark field and (b) light field.

DISCUSSION

It was already shown in previous papers (9, 20) that the grafting method enables the preparation of polymeric titanium oxide sublayers over γ-alumina for titanium loading up to 10 wt.%. The results exposed above show that these materials exhibit new properties when used as supports for platinum catalysts, in comparison with bare alumina and pure titania. In agreement with the literature (7), pure titania-supported platinum catalysts displayed a strong decrease in CO chemisorption after reduction at high

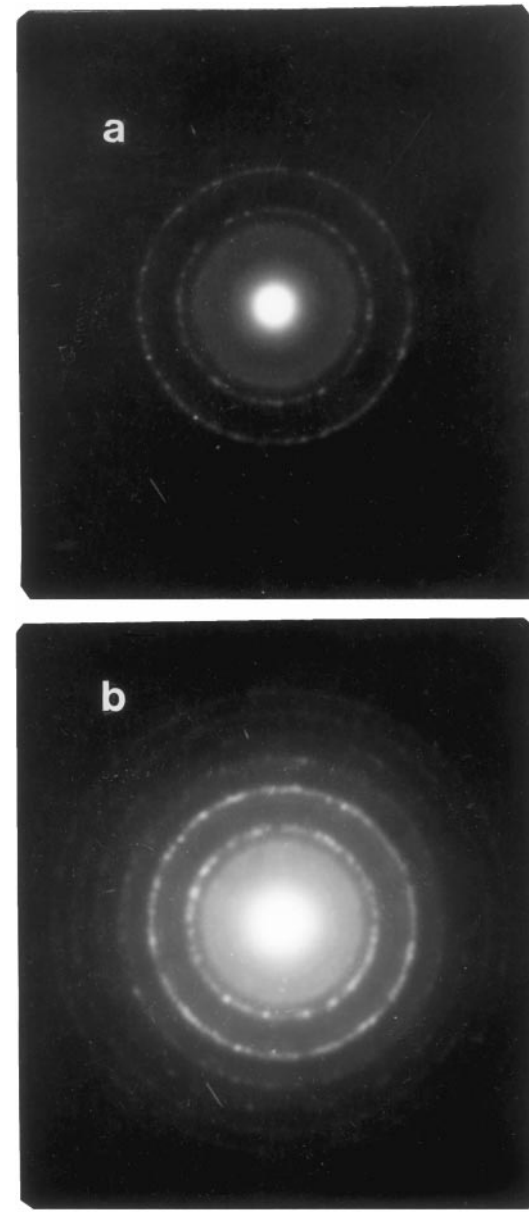

FIG. 8. The selected area electron diffraction patterns: (a) 1% Pt–10% TiO_2–Al_2O_3 (the rings are assigned to the alumina planes) and (b) 1% Pt–18% TiO_2–Al_2O_3.

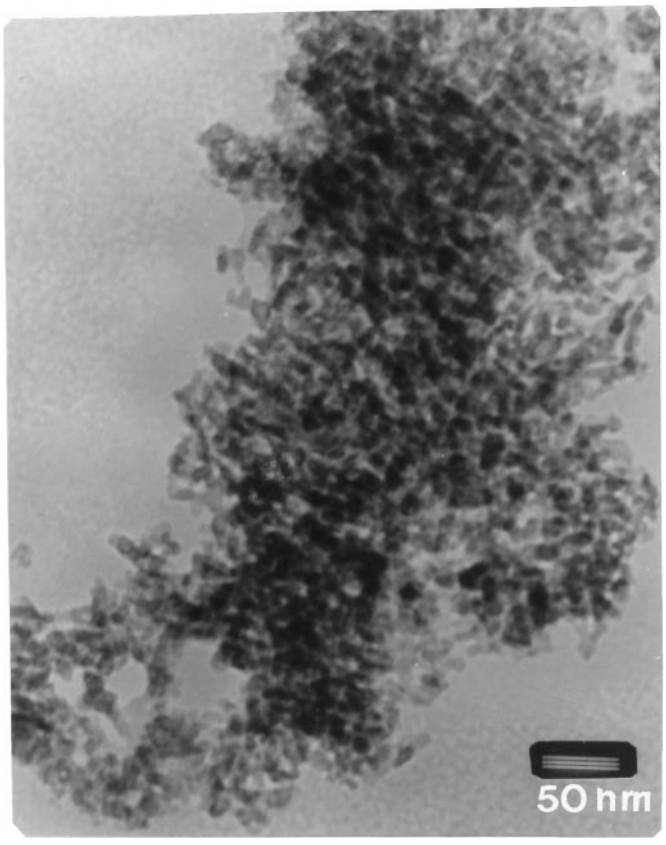

FIG. 9. TEM micrograph of the 1% Pt–18% TiO_2–Al_2O_3 catalyst.

temperature, indicating the SMSI effect. Such a decrease was not observed when alumina or alumina-grafted titanium oxides were used as supports. These results indicate that coating the alumina support with titanium oxide stabilizes the catalyst against SMSI effects.

A support with titanium loading exceeding the monolayer coverage was also prepared by impregnation with titanium isopropoxide. X-ray and electron diffraction patterns showed that anatase crystallites were present in this support. However, this observation does not exclude the possibility of some partial coating of the alumina surface by amorphous titanium oxide since the intensity of the characteristic (101) peak of the anatase phase in the XRD pattern was unexpectedly low for this high titanium loading. Platinum particles should thus be dispersed on both anatase crystallites and superficial amorphous titanium oxide. This hypothesis might justify that, as happened with alumina-grafted titanium oxides, the decrease observed in CO chemisorption after reduction at high temperature was not strong enough to correspond to a full SMSI effect.

As in the case of titania-supported platinum, partial reduction of titanium oxide was observed during the TPR experiment when both kinds of titania-modified alumina supports were used. On the other hand, the main reduction peak of the platinum phase was shifted to a lower temperature. This result suggests a synergism between platinum and titanium oxide indicating close contact of the two phases.

That platinum particles do not interact directly with the alumina surface can also be inferred from the dispersion values obtained by CO chemisorption after reduction at low temperature, which are about twice that given by alumina-supported platinum. The systematic absence of the charge transfer band at 250 nm in the DRS spectra corresponding to supports with titanium loading higher than 5 wt.% also suggests that the platinum oxide formed after calcination is already free from contact with alumina since residual oxychloride complexes are generally detected on this support.

It is thus apparent that the support prepared by impregnation, although evidencing the presence of bulk titania, behaves similarly to the grafted ones regarding platinum dispersion and reduction. Indeed, in these materials, the linkage of the titanium oxide sublayer to the alumina support stabilizes the catalyst against the SMSI effect. However, we would expect that platinum particles covering the titania crystallites in the PTA18 catalyst should exhibit the SMSI effect. This might be the case since the decrease in CO uptake after reduction at high temperature is somewhat higher in this sample than it is in catalysts prepared

TABLE 4

Average Particle Diameter (d_p) by CO Chemisorption and Transmission Electron Microscopy

	573 K[a]		773 K[a]		773 K[a]	
	Pt (%wt.)	$Sg_{Pt} \times 10^{-2}$ (m^2/g)	$d_{p\,CO}$[b] (nm)	$Sg_{Pt} \times 10^{-2}$ (m^2/g)	$d_{p\,CO}$[b] (nm)	$d_{p\,TEM}$ (nm)
PA	1.01	0.94	3.0	0.82	3.4	2.0–4.0
PTA5	1.05	1.66	1.7	1.34	2.1	2.0–3.5
PTA10	0.91	2.16	1.3	1.73	1.6	1.5–3.0
PTA18	1.02	1.60	1.8	1.18	2.4	3.0–6.0
PT	1.03	1.95	1.4	0.60	4.7	1.8–4.0

[a] After reduction in that temperature.
[b] $d_p = 6/\rho_{Pt} * Sg_{Pt}$ (19); $\rho_{Pt} = 21.45$ g/cm^3.

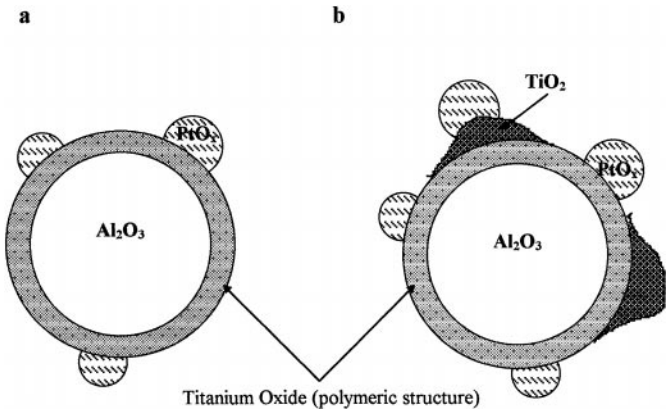

FIG. 10. Models of platinum–titanium interaction in supported catalysts dispersed on alumina: (a) up to 10% of titanium oxide and (b) above 18% of titanium oxide.

from the grafted supports. Similarly, the low H/M value obtained by frontal chemisorption is consistent with some partial SMSI effects in this catalyst. It is worth noting that reduction at RT during TPR correlates with the presence of *d–d* transition bands at about 400 nm in PT and PTA18 catalysts. These bands were attributed to bulk compounds such as $PtO_2 \cdot H_2O$ which is known to reduce easily at RT and could form preferentially on bulk titania. The smaller area of the peak at RT in the PTA18 sample suggests that only a small fraction of platinum particles covers the free titania crystallites and thus should be subject to the SMSI effect. Figure 10 summarizes the main features of this interpretation. Both grafted (Fig. 10a) and impregnated (Fig. 10b) systems display well-dispersed platinum particles over polymeric titanium oxide sublayers coating the alumina support. In addition, Fig. 10b shows the presence of some platinum particles over bulk titania for an impregnated system.

CONCLUSIONS

Highly dispersed platinum particles are obtained when polymeric titanium oxides grafted on alumina are used as supports. Grafted titanium oxides can reduce under hydrogen at high temperature but the catalysts are nonetheless stabilized against the SMSI effect. Only small morphology changes of platinum particles occur during reduction at high temperature. Supports prepared by impregnation of titanium isopropoxide with more than the equivalent monolayer exhibit both anatase crystallites and amorphous titanium oxides coating the alumina surface. The catalysts obtained by dispersion of platinum on these supports display intermediate properties between those prepared using the two kinds of materials, bulk titania and alumina-grafted titanium oxides, showing distribution of platinum between the two titanium phases. The results suggest, however, a preferential dispersion of platinum over the amorphous titanium oxide.

ACKNOWLEDGMENT

We thank CNPq (Conselho Nacional de Desenvolvimento e Pesquisa) of Brazil for supporting the authors during this work.

REFERENCES

1. Halasz, I., Brenner, A., and Shelef, M., *Appl. Catal. B* **2**, 131 (1993).
2. Harrison, B., Diwell, A., and Hallett, C., *Platinum Metal Rev.* **32**, No. 2, 73 (1988).
3. Tauster, S., Fung, S. C., and Garten, L., *J. Amer. Chem. Soc.* **100**, 170 (1978).
4. Sexton, B. A., Hughes, A. E., and Foger, K., *J. Catal.* **77**, 85 (1982).
5. Sanchez, M. G., and Gazquez, J. L., *J. Catal.* **104**, 120 (1987).
6. Herrmann, J. M., Gravelle-Rumeau-Maillot, M., and Gravelle, P. C., *J. Catal.* **104**, 136 (1987).
7. Haller, G. L., and Resasco, D. E., *Adv. Catal.* **36**, 173 (1989) (and references therein).
8. Collongues, R., "La Non-Stoechiometrie." Masson, Paris, 1971.
9. De Resende, N. S., Schmal, M., and e Eon, J.-G., "Preparation of Catalysts" (G. Poncelet *et al.*, Eds.), Vol. 6, p. 1059, Elsevier Science, Amsterdam 1995.
10. Vuurman, M. A., and Wachs, I. E., *J. Phys. Chem.* **96**, 5008 (1992).
11. Resende, N. S. de, D.Sc. Thesis, COPPE/UFRJ, Rio de Janeiro, 1995.
12. Swihart, D. L., and Mason, W. R., *Inorg. Chem.* **9**, No. 7, 1749 (1970).
13. Lietz, G., Lieske, H., Spindler, H., Hanke, W., and Völter, J., *J. Catal.* **81**, 17 (1983).
14. Lieske, H., Lietz, G., Spindler, H., and Völter, J., *J. Catal.* **81**, 8 (1983).
15. Alerasool, S., Boecker, D., Rejai, B., Gonzalez, R., del Angel, G., Azomosa, M., and Gomez, R., *Langmuir* **4**, No. 5, 1083 (1988).
16. Webb, P. A., and Orr, C., "Analytical Methods in Fine Particle Technology." Micromeritics Instrument, USA, 1997.
17. De Resende, N. S., Hernandez, T. L. A., Schmal, M., and Eon, J.-G., "Proceedings II Interamerican Congress on Electron Microscopy, Cancun, México, 1993."
18. Baker, R. T. K., Prestridge, E. B., and Garten, R. L., *J. Catal.* **59**, 293 (1979).
19. Imelik, B., et Vedrine, J., "Les Techniques Physiques d'Etude des Catalyseurs." Technip, Paris, 1988.
20. De Resende, N. S., Eon, J.-G., and Schmal, M., "Proceedings of XIV Simpósio Iberoamericano de Catalisis, Concepcion, Chile, 1994." Vol. I, p. 99.